7046 *Inorg. Chem.* **2010**, *49*, 7046–7051
DOI: 10.1021/ic1008494

Inorganic Chemistry
Article

Thermally Triggered Reversible Transformation between Parallel Staggered Stacking and Plywood-Like Stacking of 1D Coordination Polymer Chains

Jian-Ke Sun, Xu-Hui Jin, Chao Chen, and Jie Zhang*

State Key Laboratory of Structural Chemistry, Fujian Institute of Research on the Structure of Matter and Graduate School of the Chinese Academy of Sciences, Fuzhou, Fujian 350002 China

Received April 29, 2010

An unusual example showing reversible interconversion of chain-like isomers under controlled experimental settings is reported, which illustrates the key role of assembly conditions for the target packing architecture with related properties. The reaction of Mn(II) ions with an organic ligand 2-hydroxypyrimidine-4,6-dicarboxylic acid (H_3hpdc) at room temperature gives a coordination polymer $\{[Mn_3(hpdc)_2(H_2O)_6]\cdot 2H_2O\}_n$ containing parallel staggered stacking, whereas the reaction under hydrothermal conditions at 150 °C affords a compound $\{[Mn_3(hpdc)_2(H_2O)_6]\cdot H_2O\}_n$ possessing plywood-like stacking. Interestingly, two compounds contain similar one-dimensional chain components with different orientations that can be controlled by thermodynamic factors. Thermally triggered reversible interconversion of the two compounds was verified by X-ray powder, IR, and element analysis. The spin-canted antiferromagnetic behaviors are observed in as-synthesized samples, and the influence of chain orientations on magnetic properties has been detected.

Introduction

Much effort has been devoted to the design and controllable synthesis of metal−organic coordination complexes due to their potential applications in magnetism, electric conductivity, molecular adsorption, catalysis, and so on.[1] The formation of products can be influenced by temperature, solvents, pH, conformational freedom of the ligand, coordination geometry of metal ions, et al.[2] Among them, temperature is a crucial factor in determining the ultimate topology of frameworks.[3] Cheetham and co-workers provided the first systematic insight toward this aspect during their study on the formation of cobalt succinates,[4] similar observations have also been made in cobalt pyridine-3,4-dicarboxylates and zinc oxalate systems.[5] Recently, Bai and co-workers realized the control of the carboxylate coordination mode in cadmium squaric acid systems in a range of low temperatures (5−50 °C).[6] However, most temperature-dependent reactions show changes in the dimensionality of the coordination framework or mode with adjusting the temperature; the manipulation of the molecular packing patterns in a given dimension based on temperature control is less developed[7] and remains a great challenge. The infinite one-dimensional (1D) chain is the simplest topology of coordination polymers, nevertheless, its packing pattern in crystal is not simple.[8] In the most favorable case, the information of the weak noncovalent interactions, such as hydrogen bonding and $\pi-\pi$ stacking, could be stored in the low dimensions and recognized and expressed in the packing of the motifs with

*Fax: (+86) 591-8371-0051. E-mail: zhangjie@fjirsm.ac.cn.

(1) (a) Horike, S.; Shimomura, S.; Kitagawa, S. *Nat. Chem.* **2009**, *1*, 695. (b) Ma, L. Q.; Abney, C.; Lin, W. B. *Chem. Soc. Rev.* **2009**, *38*, 1248. (c) Zhang, J. P.; Huang, X. C.; Chen, X. M. *Chem. Soc. Rev.* **2009**, *38*, 2385. (d) Kim, H.; Samsonenko, D. G.; Das, S.; Kim, G. H.; Lee, H. S.; Dybtsev, D. N.; Berdonosova, E. A.; Kim, K. *Chem. Asian J.* **2009**, *4*, 886. (e) Jang, M.; Yamaguchi, T.; Ohara, K.; Kawano, M.; Fujita, M. *Chem. Asian J.* **2009**, *4*, 1524.

(2) (a) Schnatwinkel, B.; Stoll, I.; Mix, A.; Rekharsky, M. V.; Borovkov, V. V.; Inoue, Y.; Mattay, J. *Chem. Commun.* **2008**, 3873. (b) Chen, B. L.; Fronczek, F. R.; Maverick, A. W. *Chem. Commun.* **2003**, 2166. (c) Zhuang, C. F.; Zhang, J. Y.; Wang, Q.; Chu, Z. H.; Fenske, D.; Su, C. Y. *Chem.—Eur. J.* **2009**, *15*, 7578. (d) Kurmoo, M.; Kumagai, H.; Akita-Tanaka, M.; Inoue, K.; Takagi, S. *Inorg. Chem.* **2006**, *45*, 1627. (e) Hennigar, T. L.; MacQuarrie, D. C.; Losier, P.; Rogers, R. D.; Zaworotko, M. J. *Angew. Chem., Int. Ed.* **1997**, *36*, 972.

(3) (a) Forster, P. M.; Stock, N.; Cheetham, A. K. *Angew. Chem., Int. Ed.* **2005**, *44*, 7608. (b) Masaoka, S.; Tanaka, D.; Nakanishi, Y.; Kitagawa, S. *Angew. Chem., Int. Ed.* **2004**, *43*, 2530. (c) Dong, Y. B.; Jiang, Y. Y.; Li, J.; Ma, J. P.; Liu, F. L.; Tang, B.; Huang, R. Q.; Batten, S. R. *J. Am. Chem. Soc.* **2007**, *129*, 4520. (d) Harveym, H. G.; Slater, B.; Attfield, M. P. *Chem.—Eur. J.* **2004**, *10*, 3270. (e) Bernini, M. C.; Brusau, E. V.; Narda, G. E.; Echeverria, G. E.; Pozzi, C. G.; Punte, G.; Lehmann, C. W. *Eur. J. Inorg. Chem.* **2007**, 684. (f) Braga, D.; Maini, L.; Mazzeo, P. P.; Ventura, B. *Chem.—Eur. J.* **2010**, *16*, 1553. (g) Hu, C. H.; Englert, U. *Angew. Chem., Int. Ed.* **2005**, *44*, 2281.

(4) Forster, P. M.; Burbank; Livage, C.; A., R.; Férey, G.; Cheetham, A. K. *Chem. Commun.* **2004**, 368.

(5) (a) Tong, M. L.; Kitagawa, S.; Chang, H. C.; Ohba, M. *Chem. Commun.* **2004**, 418. (b) Dan, M.; Rao, C. N. R. *Angew. Chem., Int. Ed.* **2006**, *45*, 281.

(6) Zheng, B.; Dong, H.; Bai, J. F.; Li, Y. Z.; Li, S. H.; Scheer, M. *J. Am. Chem. Soc.* **2008**, *130*, 7779.

(7) (a) Sun, D.; Ke, Y.; Mattox, T. M.; Ooro, B. A.; Zhou, H. C. *Chem. Commun.* **2005**, 5447. (b) Legrand, Y. M.; van der Lee, A.; Masquelez, N.; Rabu, P.; Barboiu, M. *Inorg. Chem.* **2007**, *46*, 9083. (c) Cai, Y. P.; Zhou, X. X.; Zhou, Z. Y.; Zhu, S. Z.; Thallapally, P. K.; Liu, J. *Inorg. Chem.* **2009**, *48*, 6341.

(8) (a) Khlobystov, A. N.; Blake, A. J.; Champness, N. R.; Lemenovskii, D. A.; Majouga, A. G.; Zyk, N. V.; Schröder, M. *Coord. Chem. Rev.* **2001**, *222*, 155. (b) Lu, X. Q.; Qiao, Y. Q.; He, J. R.; Pan, M.; Kang, B. S.; Su, C. Y. *Cryst. Growth Des.* **2006**, *6*, 1910, and references therein.

Published on Web 07/07/2010

different properties.[9] Herein, we report a unique transformation between parallel staggered and plywood-like stacking of 1D coordination polymer chains. The two 1D chain-like isomers, namely $\{[Mn_3(hpdc)_2(H_2O)_6]\cdot H_2O\}_n$ **A1·H$_2$O** and $\{[Mn_3(hpdc)_2(H_2O)_6]\cdot 2H_2O\}_n$ **A2·2H$_2$O**[10a] were synthesized by varying reaction temperatures. Notably, **A2·2H$_2$O** with parallel staggered stacking pattern can be transformed to **A1·H$_2$O** with plywood-like arrangement via hydrothermal treatment or gas−solid reaction. Furthermore, **A1·H$_2$O** can be converted to **A2·2H$_2$O** based on an indirect way upon a dehydration−rehydration process. The spin-canted antiferromagnetic behaviors are observed in as-synthesized samples, and the influence of chain orientation on magnetic properties has been detected.

Experimental Section

Materials and Methods. All chemicals were obtained from commercial sources and of GR/AR grade. Fourier transform (FT) IR spectra (KBr pellets) were recorded on a Bomen MB-102 FT-IR spectrometer. Elemental analyses of C, H, and N were performed on a Vario EL III CHNOS elemental analyzer. Thermogravimetric analysis (TGA) was performed on a Mettler TGA/SDTA 851^e thermal analyzer in flowing air atmosphere at a heating rate of 10 °C·min^{-1} from 30 to 1000 °C. Powder X-ray diffraction (PXRD) patterns were recorded on Philips PW3040/60 high-resolution diffractometer at 45 kV, 40 mA for Cu Kα (λ = 1.5406 Å). The dehydrated forms of samples were prepared by heat treatment under dynamic nitrogen atmosphere at 270 °C for 2 h. Magnetic susceptibility data were measured using a Quantum Design MPMS-XL5 SQUID magnetometer. Diamagnetic corrections were made for the sample holder and the samples. The rehydrated samples for magnetic measurements were obtained by placing the dehydrated samples contained within the gelatin capsule with a small hole under water vapor atmosphere for more than two days after carrying out the magnetic measurements on the dehydrated samples.

Synthesis. $\{[Mn_3(hpdc)_2(H_2O)_6]\cdot H_2O\}_n$ **A1·H$_2$O.** 2-hydroxypyrimidine-4,6-dicarboxylic acid (H_3hpdc) was synthesized as described in the literature.[11] H_3hpdc (0.020 g, 0.11 mmol) was dissolved in 5 mL distilled water, and the pH value of the solution was adjusted to 7 with 0.05 mol/L NaOH solution. Then $MnCl_2\cdot 4H_2O$ (0.040 g, 0.2 mmol) was added to the solution and stirred for 20 min. The mixture was transferred into a 30 mL Teflon-lined autoclave and kept at 150 °C for 3 days and then slowly cooled to room temperature. Yellow block crystals of **A1·H$_2$O** obtained in 35% yield based on manganese. IR data (KBr, cm^{-1}): 3457.43(s), 1641.29(s), 1575.02(s), 1399.53(s), 1347.43(s), 1266.47(m), 1168.55(s), 1065.28(w), 928.92(w), 879.59(w), 828.91(w), 811.79(m), 787.24(m), 601.55(w), 655.77(w), 741.11(w). Anal. Calcd (%) for $C_{12}H_{16}Mn_3N_4O_{17}$ (M_r = 653.11): C, 22.07; H, 2.47; N, 8.58. Found (%): C, 22.24; H, 2.38; N, 8.74.

$\{[Mn_3(hpdc)_2(H_2O)_6]\cdot 2H_2O\}_n$ **A2·2H$_2$O.** This compound has been reported by us with in situ hydrothermal reactions of H_2cpdc (2-chloropyrimidine-4,6-dicarboxylic acid) with $MnCl_2\cdot 4H_2O$ and NaOH in aqueous solution.[10a] Here, we synthesized this compound by using a solution method at room temperature with H_3hpdc instead. The procedure was similar to that for **A1·H$_2$O**, except that the final mixture was filtered, and the filtrate was allowed to stand at room temperature for slow evaporation. Yellow prism crystals of **A2·2H$_2$O** were obtained in 30% yield on the basis of manganese after three days. IR data (KBr, cm^{-1}): 3375.25(s), 1670.57(s), 1570.02(s), 1397.49(s), 1357.23(s), 1271.59(m), 1166.26(s), 1060.40(w), 930.64(w), 880.11(w), 812.12(w), 790.97(m), 744.88(m), 648.92(w). Anal. Calcd (%) for $C_{12}H_{18}Mn_3N_4O_{18}$ (M_r = 671.12): C, 21.48; H, 2.70; N, 8.35. Found (%) for the rehydrated sample: C, 21.57; H, 2.61; N, 8.33.

X-ray crystallography. The X-ray diffraction data for **A1·H$_2$O** were collected on a Rigaku SCXmini CD diffractometer with graphite-monochromated Mo Kα radiation (λ = 0.71073 Å) at 293 K. The CrystalClear program was used for the absorption correction. The structure was solved by direct methods with SHELXS-97 and refined by full-matrix least-squares fitting on F^2 by SHELXL-97. All nonhydrogen atoms were refined anisotropically. The hydrogen atoms on the carbon atoms were placed in calculated positions with isotropic displacement parameters set to 1.2Ueq of the attached atoms. The hydrogen atoms of coordinated water molecules as well as lattice water molecules were first determined in difference Fourier syntheses and then fixed at the calculated positions. The selected bond distances and angles of the two compounds are listed in Table S1 in the Supporting Information.

Crystal data for **A1·H$_2$O**: $C_{12}H_{16}Mn_3N_4O_{17}$, monoclinic, space group $C2/c$, a = 15.621(2), b = 10.6503(9), c = 12.1608(14), V = 2021.3(4), Z = 4, μ = 1.947 mm^{-1}, Dc = 2.146 g cm^{-3}, S = 1.062, R = 0.0320, and wR = 0.0824 for 2042 independent reflections [$I > 2\sigma(I)$]. CCDC-770532 contains the supplementary crystallographic data for this paper.

Results and Discussions

Structural Descriptions. Single crystal X-ray diffraction analysis reveals that the asymmetry unit of **A1·H$_2$O** contains two crystallographically unique Mn atoms, one $hpdc^{3-}$ anion, three coordinated water molecules, and a half of lattice water molecule that resides on the special position. The Mn2 atom, located on a crystallographic inversion center, is connected to two symmetry-related Mn1 atoms via the μ_2-carboxylate O atom and the −OCN− species of $hpdc^{3-}$ ligand to form a trinuclear unit, which is held together through double −OCN− bridges, giving rise to a 1D coordination polymer chain with the remaining coordination sites on the metals being occupied by water molecules (Figure 1). Interestingly, the coordination sphere and linkage modes of metal ions within 1D chains of **A1·H$_2$O** is similar to that of **A2·2H$_2$O**,[10a] with a small discrepancy in the bond lengths and angles (see Table S1 in the Supporting Information). However, the chain packing modes in two complexes are remarkably different (Figure 2). In **A1·H$_2$O**, there are two sets of chains that are arranged in two different directions with a torsion angle of 45.76°, one extends along the [1,−1,0] direction and the other along the [1,1,0] direction. Finally these two sets of chains interconnect with each other by interchain hydrogen bonds and alternately stack along the [0,0,1] direction in a −ABAB− fashion to form a plywood-like array, which is less common in crystal engineering. Whereas in **A2·2H$_2$O**,[10a] there is only one set of chains that runs along the [0,0,1] direction. Extensive hydrogen bonds connect adjacent chains to form a parallel staggered stacking.

(9) (a) Yao, Q. X.; Ju, Z. F.; Jin, X. H.; Zhang, J. *Inorg. Chem.* **2009**, *48*, 1266. (b) Carlucci, L.; Ciani, G.; Gramaccioli, A.; Peoserpio, D. M.; Rizzato, S. *CrystEngComm* **2000**, 154. (c) Tong, M. L.; Chen, H. J.; Chen, X. M. *Inorg. Chem.* **2000**, *39*, 2235. (d) Li, Y. H.; Su, C. Y.; Goforth, A. M.; Shimizu, K. D.; Gray, K. D.; Smith, M. D.; zur Loye, H. C. *Chem. Commun.* **2003**, 1630. (e) Wu, C. D.; Lin, W. B. *Angew. Chem., Int. Ed.* **2005**, *44*, 1958. (f) Lee, E. Y.; Suh, M. P. *Angew. Chem., Int. Ed.* **2004**, *43*, 2798. (g) Zhang, J.; Matsushita, M. M.; Kong, X. X.; Abe, J.; Iyoda, T. *J. Am. Chem. Soc.* **2001**, *123*, 12105. (h) Cheng, A. L.; Ma, Y.; Zhang, J. Y.; Gao, E. Q. *Dalton Trans.* **2008**, 1993.

(10) (a) Jia, H. P.; Li, W.; Ju, Z. F.; Zhang, J. *Chem. Commun.* **2008**, 371. (b) Gao, E. Q.; Wang, Z. M.; Yan, C. H. *Chem. Commun.* **2003**, 1748. (c) Ko, H. H.; Lim, J. H.; Kim, H. C.; Hong, C. S. *Inorg. Chem.* **2006**, *45*, 8847.

(11) Schmalzi, K. J.; Sharma, S. C.; Christopherson, R. I. 2-oxo-4-carboxy-pyrimidines and their use as anti-malaria and anti-cancer agents. US. Pat. 4873228, October 10, 1989.

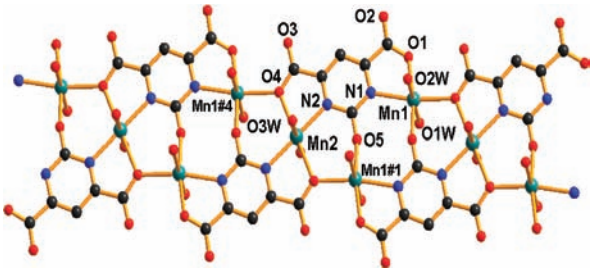

Figure 1. The 1D chain in **A1·H$_2$O**. Atom with #1 and #4 are symmetrically generated. All hydrogen atoms and lattice water molecules are omitted for clarity.

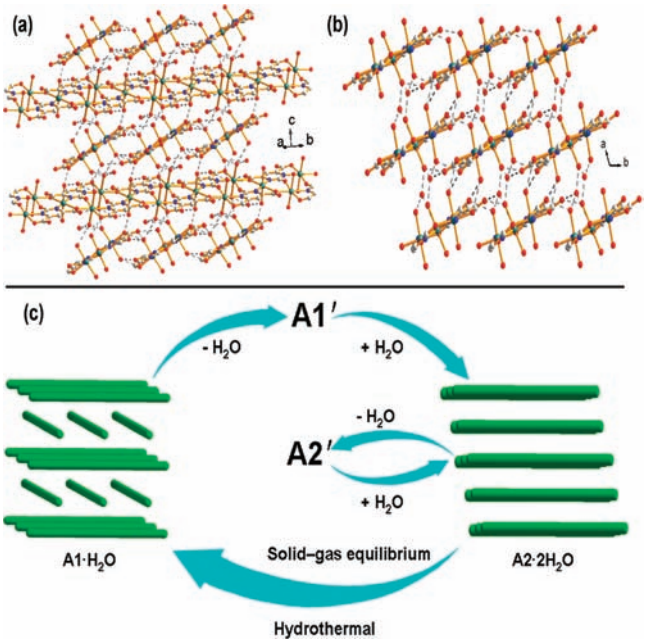

Figure 2. Ball-and-stick representation of the packing patterns for (a) **A1·H$_2$O** and (b) **A2·2H$_2$O**, respectively. The gray broken lines represent hydrogen bonds. Hydrogen atoms are omitted for clarity. (c) Schematic illustrations of the transformation between the plywood-like stacking in **A1·H$_2$O** and the parallel staggered stacking in **A2·2H$_2$O**. The 1D chains in **A1·H$_2$O** and **A2·2H$_2$O** are represented by green rods, and the interchain lattice water molecules are omitted for clarity. **A1′** and **A2′** represent the two kinds of different amorphous phases after dehydration of **A1·H$_2$O** and **A2·2H$_2$O**.

Reversible Structural Transformation. During the temperature-controlled synthesis of metal−organic frameworks, the changes in the coordination geometry of metal ions and the bonding mode of ligands as well as the dimensionality of the coordination framework are more common.[4−6] However, the temperature change in our case exerts only a great influence on the number of noncoordinated water molecules in the crystal lattice, which result in two structures with different densities (densities for **A2·2H$_2$O** and **A1·H$_2$O** are 2.061 and 2.146 g·cm^{-3}, respectively). The nearest interchain Mn···Mn distance in **A2·2H$_2$O** is 5.836 Å whereas in **A1·H$_2$O** is 5.662 Å. With the decrease of the distance between adjacent chains, the lattice water molecules move away from a normal position to a special position, reaching a compromise with their corresponding packing geometry of the chains. The orientations of interchain hydrogen bonds show a trend that is concomitant with the arrangement of chains, suggesting a cooperative effect of hydrogen bonding in directing and stabilizing the two distinct packing modes in **A1·H$_2$O** and **A2·2H$_2$O**, respectively. The isolation of denser structures at higher temperature clearly suggests that the process is influenced by thermodynamic factors; the amount of water involved in the final structure decreases with increasing temperature, verifying the process is entropy favorable ($\triangle S > 0$).[4,12]

The plywood-like arrangement is ubiquitous in our daily lives owing to their high strength and stability. However, the parallel stacking pattern of the chains is overwhelmingly predominant over the nonparallel fashion with cross-like arrangement in the field of crystal engineering of metal−organic systems. Although such a nonparallel array may deliver some unique characteristics to the crystal, such as anisotropic properties or porosity depending on orientation of the chains,[8,9] little exploration on the origin of this orientation preference and the possibility of structural manipulation has been made. Can the interchain arrangement be adjusted by an external driving force without destroying the coordination skeletons? Different orientations of the similar 1D chains in the two isomers obtained at different temperature inspire us to search for a transformation between parallel staggered and plywood-like stacking. When some crystals of **A2·2H$_2$O** were put directly into an autoclave containing distilled water and heated at 150 °C for 24 h, to our surprise, **A2·2H$_2$O** can be totally transformed to **A1·H$_2$O**, as confirmed by PXRD (Figure 3). Further, the conversion experiment was designed deliberately based on the consideration of gas−solid equilibrium under hydrothermal conditions. An open tube containing the crystals of **A2·2H$_2$O** (no water in the tube) was confined in a sealed autoclave with water and allowed to stand for 16 h at 150 °C. The PXRD pattern of the final phase indicates that **A2·2H$_2$O** could be completely transformed to **A1·H$_2$O** via a solid−solid transformation process. This result is fascinating because it provides an unusual example of the structural transformation via twisting the chains to a different orientation based on thermodynamics approach, which is meaningful for the chemists in rational design of switchable functional materials.

Although heat-treatment can transform the parallel stacking to the plywood-like stacking, the inverse transformation from **A1·H$_2$O** to **A2·2H$_2$O** (water vapor undergoes inclusion into crystal state, $\Delta S < 0$) cannot be realized directly by cooling treatment, even cooling the sample to liquid nitrogen temperature. This can be easily understood since a reaction that is thermodynamically feasible may not be kinetically favorable. Interestingly, when we destroyed the interchain hydrogen bonds of two compounds by heating the sample at 270 °C to remove all water molecules (TGA in Supporting Information, Figure S1) and then exposed the dehydrated samples **A1′** and **A2′** to moist atmosphere, **A1′** could be spontaneously transformed to **A2·2H$_2$O** after 24 h, as verified by PXRD (Figure 3), IR (Figure 4), and element analysis,[13] although it undergoes a little loss in crystallinity. The reversible

(12) (a) Mahata, P.; Sundaresan, A.; Natarajan, S. *Chem. Commun.* **2007**, 4471. (b) Mahata, P.; Prabu, M.; Natarajan, S. *Inorg. Chem.* **2008**, *47*, 8451.

(13) Element analysis for **A2·2H$_2$O** ($C_{12}H_{18}Mn_3N_4O_{18}$) calcd (%): C, 21.48; H, 2.70; N, 8.35. Rehydrated **A1′** sample, found (%): C, 21.45; H, 2.70; N, 8.41.

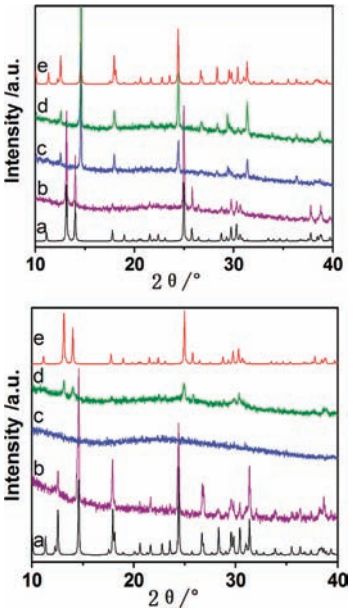

Figure 3. PXRD patterns showing the transformation from **A2·2H$_2$O** to **A1·H$_2$O** (top) and **A1·H$_2$O** to **A2·2H$_2$O** (bottom). Top: (a) calculated powder pattern of **A2·2H$_2$O,** (b) experimental powder pattern of **A2·2H$_2$O**, (c) crystals **A2·2H$_2$O** were put into autoclave with water and kept at 150 °C for 24 h, (d) open tube with some crystals of **A2·2H$_2$O** (no water in the tube) was confined in an autoclave containing water and kept at 150 °C for 16 h, and (e) calculated powder pattern of **A1·H$_2$O**. Bottom: (a) calculated powder pattern of **A1·H$_2$O**, (b) experimental powder pattern of **A1·H$_2$O**, (c) **A1·H$_2$O** dehydrated at 270 °C to obtain amorphous phase **A1′**, (d) sample after exposure to a H_2O vapor, and (e) calculated powder pattern of **A2·2H$_2$O**.

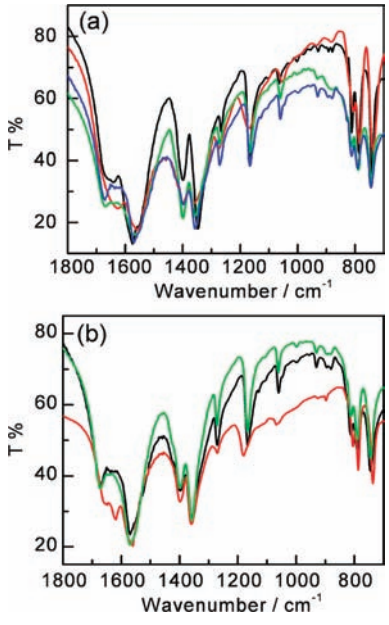

Figure 4. (a) IR spectra recorded for the transformation from **A1·H$_2$O** to **A2·2H$_2$O**; **A1·H$_2$O** (black), **A1′**(red), **A1′**-rehydrated (green), and **A2·2H$_2$O**(blue). (b) IR spectra recorded for the transformation from **A2′** to **A2·2H$_2$O**; **A2·2H$_2$O** (black), **A2′** (red), and **A2′**-rehydrated (green).

transformation from **A2′** to **A2·2H$_2$O** was observed (Supporting Information, Figure S2). These observations indicate that the **A2·2H$_2$O** should be a more stable phase at low temperature, in this case, the parallel stacking as an energetically favored configuration occurs preferentially. In recent years, the structural transformations of metal−organic coordination complexes induced by thermal treatment or desolvation have attracted considerable attention.[14] A number of interesting examples involving single-crystal to single-crystal[15] or crystal to amorphous to crystal transformations[16] have been reported. Among them, the changes in the coordination mode, thermal association or condensation, rearrangement of bonds, or distortion and sliding of network structures were already observed. For 1D coordination polymer chains, although various types of packing arrays can be constructed under different experimental conditions,[8,9] such a reversible manipulation of the chain orientations based on thermal treatment accompanied by dehydration/hydration is rarely reported.

After dehydration, most absorption bands in the IR spectra of two samples coincide with those in the as-synthesized samples except for some frequency shifts (Figure 4), suggesting that the $Mn_3(hpdc)_2$ coordination skeletons of polymer chains are remaining in **A1′** and **A2′**. This high stability may be related to the special chelating ability of the $hpdc^{3-}$ ligand. However, one question may be raised at this point. After the hydrogen bonds are broken, does a difference in chain orientation still remain? Although the formation of amorphous state increases the difficulty in the structural analysis on two dehydrated samples, the magnetic study of these two samples offers a significant insight into understanding the effects of different chain orientations.

Structural-Related Magnetic Properties. Magnetic studies reveal that **A1·H$_2$O** exhibits a similar spin-canted antiferromagnetic behavior to that of **A2·2H$_2$O**.[10a] Under an external field of 5 kOe, the $\chi_m T$ value decreases smoothly to ca. 75 K and then drops quickly to 4.81 cm^3 K mol^{-1} at 4 K with decreasing temperature. Below 4 K, the $\chi_m T$ curve shows a small rise, which is field dependent and disappears at a higher field (Figure 5a). Such behavior is characteristic of spin-canted antiferromagnetism. The antisymmetric exchange between the Mn^{II} centers and the slanted equatorial planes of Mn^{II} ions within the chain, as that observed in **A2·2H$_2$O**, should be mainly responsible for this canting effect.[10a] Taking into account the structural characters of the 1D chain, an approximate fit to the magnetic susceptibility data was achieved based on a model for linear Mn^{II} trimers (J), where a molecular field approximation (zJ')

(14) (a) Vittal, J. J. *Coord. Chem. Rev.* **2007**, *251*, 1781. (b) Kawano, M.; Fujita, M. *Coord. Chem. Rev.* **2007**, *251*, 2592. (c) Ganguly, R.; Sreenivasulu, B.; Vittal, J. J. *Coord. Chem. Rev.* **2008**, *252*, 1027. (d) Noro, S.; Kitagawa, S.; Akutagawa, T.; Nakamura, T. *Prog. Polym. Sci.* **2009**, *34*, 240, and references therein.

(15) (a) Ghosh, S. K.; Kaneko, W.; Kiriya, D.; Ohba, M.; Kitagawa., S. *Angew. Chem., Int. Ed.* **2008**, *47*, 8843. (b) Yoshida, Y.; Inoue, K.; Kurmoo, M. *Inorg. Chem.* **2009**, *48*, 10726. (c) Zhang, Y. J.; Liu, T.; Kanegawa, S.; Sato, O. *J. Am. Chem. Soc.* **2010**, *132*, 912. (d) Mobin, S. M.; Srivastava, A. K.; Mathur, P.; Lahiri., G. K. *Dalton Trans.* **2010**, *39*, 1447. (e) Sadeghzadeh, H.; Morsali, A. *Inorg. Chem.* **2009**, *48*, 10871. (f) Duan, Z. M.; Zhang, Y.; Zhang, B.; Zhu, D. B. *J. Am. Chem. Soc.* **2009**, *131*, 6934. (g) Kim, T. H.; Shin, Y. W.; Jung, J. H.; Kim, J. S.; Kim, J. *Angew. Chem., Int. Ed.* **2008**, *47*, 685. (h) Aslani, A; Morsali, A. *Chem. Commun.* **2008**, 3402.

(16) (a) Ghosh, S. K.; Azhakar, R.; Kitagawa, S. *Chem. Asian J.* **2009**, *4*, 870. (b) Zhang, J. P.; Kitagawa, S. *J. Am. Chem. Soc.* **2008**, *130*, 907. (c) Roques, N.; Maspoch, D.; Imaz, I.; Datcu, A.; Sutter, J.-P.; Rovira, C.; Veciana, J. *Chem. Commun.* **2008**, 3160. (d) Yoshida, Y.; Inoue, K.; Kurmoo, M. *Inorg. Chem.* **2009**, *48*, 267.

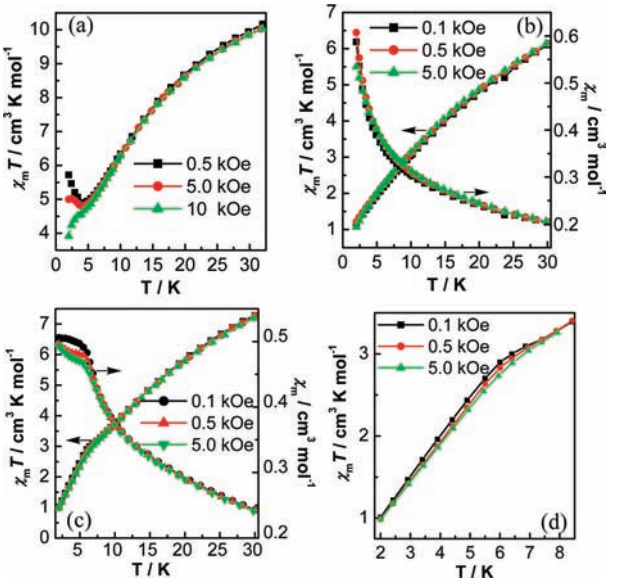

Figure 5. (a) The $\chi_m T$ vs T plots under different fields at low temperature for **A1**·$\mathbf{H_2O}$. (b) The $\chi_m T$ vs T and χ_m vs T plots under different fields at low temperature for dehydrated sample **A1′**. (c) The $\chi_m T$ vs T and χ_m vs T plots under different fields at low temperature for dehydrated sample **A2′**. (d) Magnified $\chi_m T$ vs T plots under different fields for **A2′** in the range of 2−8.5 K.

was considered for intertrimer interactions. The best fitting parameters are $J = -0.88$ cm^{-1}, $zJ' = +0.02$ cm^{-1}, and $g = 2.02$ (Supporting Information, Figure S3).

For dehydrated sample **A1′**, the χ_m and $\chi_m T$ product exhibit a monotonous increase and decrease upon cooling, respectively. The absence of magnetic field dependence and no abrupt increase in the $\chi_m T$ value at low temperature (Figure 5b) suggests the disappearance of a spin-canting effect upon dehydration. A least-squares fit of the magnetic susceptibility data, based on the abovementioned model, led to the values of $J = -1.57$ cm^{-1}, $zJ' = -0.47$ cm^{-1}, and $g = 2.03$ (Supporting Information, Figure S3), revealing a slight enhancement of antiferromagnetic coupling interactions in **A1′**. Interestingly, the dehydrated sample **A2′** exhibits a magnetic property which is different from that of **A1′**. With lowering temperature, the χ_m value increases steadily to reach an inflection point at about 6 K. Below this temperature, the χ_m value increases slowly and is field dependent (Figure 5c). The $\chi_m T$ vs T curves at different applied fields show the appearance of a very small spontaneous magnetization below 6.5 K along with a small increase in $\chi_m T$ values as the applied field decreases, which implies the existence of a canted antiferromagnetic state (Figure 5d). These distinct magnetic behaviors at low temperature clearly reveal that the two dehydrated samples possess different structural characteristics. When **A1′** and **A2′** were rehydrated, the primordial magnetic behaviors can be recovered (Supporting Information, Figure S4). In this case, it should be noted that the magnetic behavior of the rehydrated **A1′** corresponds to that of **A2**·$\mathbf{2H_2O}$.

For both isomers **A1**·$\mathbf{H_2O}$ and **A2**·$\mathbf{2H_2O}$, the spin-canted antiferromagnetism is observed. Due to the isotropic character of the high-spin Mn^{II} ion, the existence of the slanted basal planes of adjacent Mn^{II} ions should be responsible for this canting effect.[10] When the two compounds are totally dehydrated, only the $Mn_3(hpdc)_2$ coordination skeleton is kept in **A1′** and **A2′**. The difference in magnetic behavior of the dehydrated samples clearly shows the effect of chain orientations. For **A1′,** the plywood-like stacking hampers the migration of the 1D chains, therefore, no significant interchain interaction may take place upon dehydration. The departure of the axial water molecules brings about a configuration modification from twist to flatness, resulting in the disappearance of a spin-canting effect. For **A2′,** the 1D chains packing as parallel bundles are less affected by steric hindrance. The removal of coordinated water allows the formation of the axial Mn−O interactions involving the oxygen atoms of carboxylate groups of neighboring chains through interchain aggregation, which may induce the structural deformation of the chain skeleton and facilitate the formation of high-dimensional framework. Therefore, a different magnetic behavior from that of **A1′** can be found. From IR spectra, it can be found that a new intense and broad band appeared at 1618.29 cm^{-1} in **A2′** (Figure 4), except that the characteristic $\nu_{as}(COO^-)$ vibrations of both compounds shift to a low wavenumber after dehydration. This observation clearly shows the difference of a carboxylate bridging mode in **A1′** and **A2′**, supporting the axial coordination of carboxylate oxygen atoms.[17] Up to date, the solvent-induced structural and magnetic conversion has attracted intense interest,[18] and several interesting examples have shown that a condensation process of the low-dimensional skeleton into the high-dimensional system may occur after the loss of the coordinated water molecules in order to maintain the octahedral environment of the metal ion.[19] Our results demonstrate an important influence of skeleton orientation on such a process and suggest a potential pathway for manipulating skeleton orientation.

Conclusion

The present studies describe a thermal dehydration-assisted packing isomerization of one-dimensional (1D) coordination polymer chains. A reversible phase transformation between parallel staggered and plywood-like stacking of chains can be completed in multiple ways, such as solution, solid to solid, or crystalline to amorphous to crystalline processes. These results not only provide a new insight into understanding the intrinsic connection of packing geometry of different structures but also are intriguing for further design and synthesis of advanced functional materials.

Acknowledgment. This work was supported by the National Natural Science Foundation of China (nos.

(17) (a) Michaelides, A.; Skoulika, S. *Cryst. Growth Des.* **2005**, *5*, 529. (b) Skoulika, S.; Dallas, P.; Siskos, M. G.; Deligiannakis, Y.; Michaelides, A. *Chem. Mater.* **2003**, *15*, 4576. (c) Pan, L.; Zheng, N. W.; Wu, Y. G.; Han, S.; Yang, R. Y.; Huang, X. Y.; Li, J. *Inorg. Chem.* **2001**, *40*, 828.

(18) (a) Yanai, N.; Kaneko, W.; Yoneda, K.; Ohba, M.; Kitagawa, S. *J. Am. Chem. Soc.* **2007**, *129*, 3496. (b) Chen, X. D.; Zhao, X. H.; Chen, M.; Du, M. *Chem.—Eur. J.* **2009**, *15*, 12974. (c) Zhang, Y. J.; Liu, T.; Kanegawa, S.; Sato, O. *J. Am. Chem. Soc.* **2009**, *131*, 7942.

(19) (a) Masciocchi, N.; Galli, S.; Tagliabue, G.; Sironi, A.; Castillo, O.; Luque, A.; Beobide, G.; Wang, W. G.; Romero, M. A.; Barea, E.; Navarro, J. A. R. *Inorg. Chem.* **2009**, *48*, 3087. (b) Cheng, X. N.; Zhang, W. X.; Chen, X. M. *J. Am. Chem. Soc.* **2007**, *129*, 15738.

20973171/20671090) and the Key Project from the Chinese Academy of Sciences (KJCX2.YW.H01).

Supporting Information Available: X-ray crystallographic files in CIF format, PXRD patterns of reversible dehydration−rehydration processes of $\mathbf{A2 \cdot 2H_2O}$, TG plots of two compounds, the related magnetic plots, and magnetic model as well as selected bonds and angles of the two compounds. These materials are available free of charge via the Internet at via the Internet at http://pubs.acs.org.